Paper

Int'l J. of Aeronautical & Space Sci. 16(4), 571–580 (2015)
DOI: http://dx.doi.org/10.5139/IJASS.2015.16.4.571

IJASS
International Journal of Aeronautical and Space Sciences

Rotor Blade Sweep Effect on the Performance of a Small Axial Supersonic Impulse Turbine

Sooin Jeong*

Industrial Liaison Innovation Center, Pusan National University, Busan 46241, Republic of Korea

Byoungik Choi**

Rolls-Royce University Technology Center in Thermal Management, Pusan National University, Busan 46241, Republic of Korea

Kuisoon Kim***

Department of Aerospace Engineering, Pusan National University, Busan 46241, Republic of Korea

Abstract

In this paper, a computational study was conducted in order to investigate the rotor blade sweep effect on the aerodynamics of a small axial supersonic impulse turbine stage. For this purpose, three-dimensional unsteady RANS simulations have been performed with three different rotor blade sweep angles (-15°, 0°, +15°) and the results were compared with each other. Both NTG (No tip gap) and WTG (With tip gap) models were applied to examine the effect on tip leakage flow. As a result of the simulation, the positive sweep model (+15°) showed better performance in relative flow angle, Mach number distribution, entropy rise, and tip leakage mass flow rate compared with no sweep model. With the blade static pressure distribution result, the positive sweep model showed that hub and tip loading was increased and midspan loading was reduced compared with no sweep model while the negative sweep model (-15°) showed the opposite result. The positive sweep model also showed a good aerodynamic performance around the hub region compared with other models. Overall, the positive sweep angle enhanced the turbine efficiency.

Key words: Supersonic turbine, Swept rotor blade, Unsteady flow, Turbine performance

1. Introduction

The performance of axial flow turbomachinery has been continually improved for decades. The three-dimensional blading technique of a conventional subsonic or transonic turbine such as sweep and lean is the one of these topics as well as endwall contouring and streamwise endwall fence for reducing the loss. From early 1950s, many researches on the swept blade effect of axial flow turbomachinery design have been conducted. Lewis and Hill [1] demonstrated the influence of sweep and dihedral on the meridional flows of a turbine cascade by means of theoretical method. Later on, Hill and Lewis [2] presented the experimental investigations for the swept turbine nozzle cascade compared with their theoretical calculations. They concluded that the end effects had been observed for swept blade and strong streamline shifts of the meridional flow also had been observed which cause the Bernoulli surfaces to twist as the flow proceeds through the blade passage. Denton and Xu [3] described fully 3D flow effects of blade sweep, lean and localized twist to improve axial turbo-machine performance. They showed how the blade loading changes due to sweep near the end wall. The possibility of shock loss reduction was shown for transonic compressor or fan using the blade sweep in design. They, however, also concluded that the net effect on overall loss was not obvious because of an extra pressure rise by

* Researcher
** Researcher
*** Professor, Corresponding author: kuskim@pusan.ac.kr

Received: September 15, 2015 Revised: December 9, 2015 Accepted: December 10, 2015

http://ijass.org pISSN: 2093-274x eISSN: 2093-2480

diffusion which will generate extra boundary layer losses.

Meanwhile, blade sweep has been used in transonic fan and compressor design with the intent of reducing shock losses, analogous to the use of swept wings in external aerodynamic applications. In 1998, Wadia et al. [4] reported the experimental and analytical assessment of the effect of aft- and forward sweep technology of transonic fan or compressor rotors. They concluded that forward sweep can result in improvements in both efficiency and stall margin and the better performance of the forward-swept rotor is attributed to the reduced shock/boundary layer interaction resulting from reduced axial flow diffusion. Gümmer et al. [5] described the aerodynamic endwall effects of sweep and dihedral for highly loaded transonic compressor stators. Their results showed that the advanced blade improved radial distribution of loading and development of three-dimensional endwall boundary layers. Denton [6] investigated the effects of sweep on transonic fan performance to find out the pros and cons of sweep. He figured out that reduced shock loss could be induced by 3D design such as sweep but this is usually at the expense of reduced stall margin and increased loss elsewhere along the blade span. In recent years, Pullan and Harvey [7], [8] examined the influence of sweep at midspan and endwall of a high aspect ratio turbine blade row and found that the spanwise velocity component does not contribute to blade loading. They observed the midspan profile loss rose with increasing sweep. It is also shown that sweep causes the blade to become more rear loaded at the hub and fore loaded at the casing. Yoon et al. [9] examined the non-orthogonal IP turbine stator that incorporates sweep numerically and experimentally. They showed that the non-orthogonal stator reduces the flow diffusion between the stator and rotor.

The three-dimensional blade design in numerical researches carried out so far is, however, limited to subsonic or transonic fan/compressor using steady-state calculation. But the steady-state calculation has its limits because the turbine efficiency can vary up to 1% or more depending on the relative position of nozzle wake and rotor inlet. In addition, numerical models with various sweep angles necessarily cause different nozzle-rotor axial spacing along the span. That is, the relative position of nozzle wake and rotor inlet couldn't be kept the same. These days, unsteady-state calculation studies have steadily been increased on this topic. Lately, Hah and Shin [10] investigated the detailed near-stall flow behavior in a modern transonic fan with a compound sweep using both URANS and LES methods. In their research, the compound sweep toward the rotor tip contributes to the flow structure at the rotor tip more stable compared to that of the conventional blade design.

There have been few known researches on the swept rotor blade effect for a supersonic impulse turbine. Moreover, the unsteady analysis of supersonic impulse turbine with swept rotor blade can hardly be found so far. In this paper, three-dimensional unsteady RANS (URANS) simulations was performed on the small supersonic axial turbine having backward/forward rotor blade sweep angles (±15°) including no sweep angle (0°) as a datum. The time-averaged performance results were compared with each other in order to investigate the effect of rotor blade sweep angle on a supersonic impulse turbine aerodynamics. Both NTG (No tip gap) and WTG (With tip gap) models were applied to examine the effect on tip leakage mass flow rate.

2. Numerical Method

2.1 Model Turbine Geometry

Turbine model used for this study is a partial admission supersonic axial turbine consists of 21 convergent-divergent nozzles having rectangular shaped exit and 100 impulse type rotor blades shown in Fig.1. Both "No tip gap" case (NTG) and "With tip gap" case (WTG) with shrouded type rotor blade were adopted. The inlet total to outlet static pressure ratio is 18.34. The exit velocity of nozzle is designed to reach Mach 2.33. As shown in Fig.2, rotor blades have some hub and tip overlaps for performance improvement. For the effective calculation, 1/25 annulus model (1 nozzle + 4 rotors passages) with rotational periodic boundary condition was

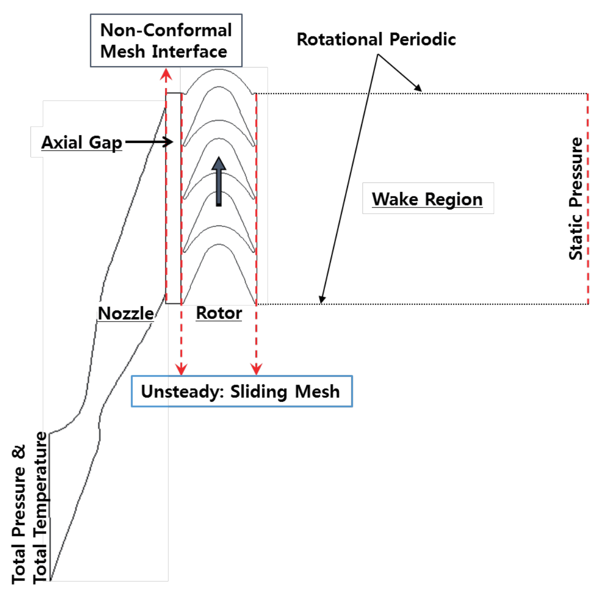

Fig. 1. Turbine geometry at midspan and numerical boundary conditions

utilized as shown in Fig. 1. For the WTG cases, the flat blade tip is modeled with a tip gap of approximately 9% of the blade height.

2.2 Blade Sweep Models

Blades are said to have sweep when the axisymmetric stream surface is not perpendicular to the spanwise direction [9]. The definition of sweep angle is illustrated in Fig. 3. Three sweep angle models were designed and simulated for both of NTG and WTG in this study. Including no sweep model (NSW, sweep angle 0°), the basis for comparison, backward sweep (BSW, sweep angle +15°) and forward sweep (FSW, sweep angle -15°) model were analyzed. The schematics of six computational cases are shown in Fig.4.

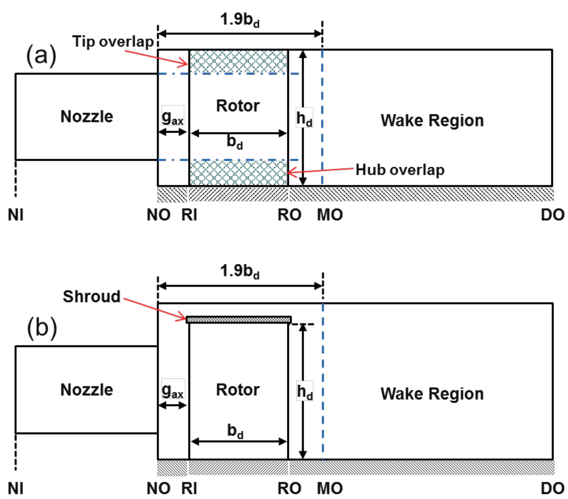

Fig. 2. Schematics of turbine side view (a) No tip gap, NTG (b) With tip gap, WTG

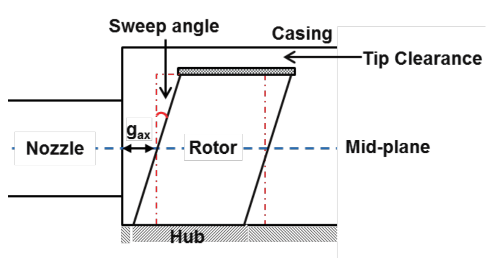

Fig. 3. Definition of sweep angle

2.3 Numerical Method

Three-dimensional unsteady RANS (URANS) simulation has been performed. All numerical analyses were carried out by using FLUENT with density-based coupled solver. Quantities at cell faces of finite volumes are discretized with 2nd-order upwind scheme and 2nd-order implicit method were adopted for temporal discretization. Turbulence was modeled using k-ω SST model developed by Menter [11]. The y^+ values at all wall boundaries are set to be less than 5. Boundary conditions and interface types used in this study are shown in Fig. 1. Turbine inlet conditions for all tests were set to dry air at total pressure (1.95MPa) and total temperature (373K). The domain outlet boundary condition was specified with the static pressure (0.1MPa). Rotational speed of the rotor is 6147.5 RPM. The Sliding mesh model (SMM) was utilized at each stationary-rotational interface for unsteady calculation. The time period of the unsteadiness(τ) is defined as the time required for the rotation of one rotor pitch and the time step(Δt) can be determined by dividing the time period by the number of time steps in a period. In this paper, 50 time steps in one rotor passage were selected by the time step independency test. So the time step of $\Delta t = 1.952\times10^{-06}$ s was chosen, finally. The surface grids and grids inside midspan for turbine stage can be seen in Fig. 5. Total numbers of grids are about 1.48million for NTG model and about 1.75 million for WTG model.

In order to validate the numerical model adopted in this study, the computational result of equivalent specific work with pressure ratio is compared with the experimental results of a single-stage turbine with a rotor entering relative Mach

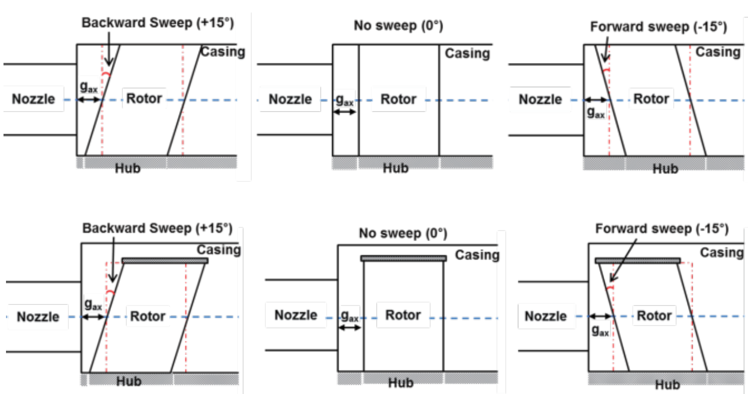

Fig. 4. Computational cases (Backward sweep, +15°, No sweep, 0°, Forward Sweep, -15°)

number of two which have been reported by Moffitt[12] and Moffitt and Klag[13] in Fig. 6. The computational result of this study shows the comparable trend of the experimental result.

3. Results

3.1 Sweep effect on the incidence

In Fig. 7, the mass-averaged values of time-mean incidence angles at rotor inlet (i) and deviation angles at rotor outlet (δ) are plotted. As can be seen from the figure, the positive incidence or deviation implies that the relative flow angle is smaller than the blade angle with respect to tangential line. The incidences of NSW(0°) models observed from the calculation are about positive 3 degree. The incidence angles at rotor inlet (RI) plane show a large variation with sweep angle. The result of BSW(+15°) model shows smaller incidence angle compared with that of NSW model in both NTG and WTG cases. The incoming flow of FSW(-15°) model is much more turned toward turbine rotational direction compared with NSW model. At rotor outlet (RO) plane, the deviation angle of FSW model is little less than those of other two models while the deviation angles of BSW and NSW model are very similar.

The incidence angle in supersonic blade is a very important parameter related to source of turbine losses such as flow separation on the blade suction surface and shock waves, so it is necessary to keep close to zero as possible. In order to observe the change of flow incidence with spanwise direction in more detail, the circumferentially averaged values of incidence angle along the span are presented in Fig. 8. First, in NSW model, the incidence distribution is comparatively close to zero incidence line within 15%~80% of span which coincides with the height of nozzle outlet, whereas the incidence angles have considerable discrepancies in hub and tip overlap region. The FSW model displays the incidence angle becomes bigger as the per cent

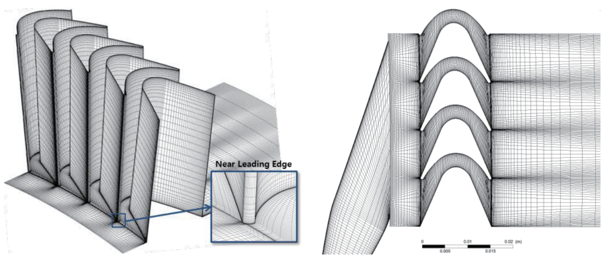

Fig. 5. Surface grid and grid of mid-span

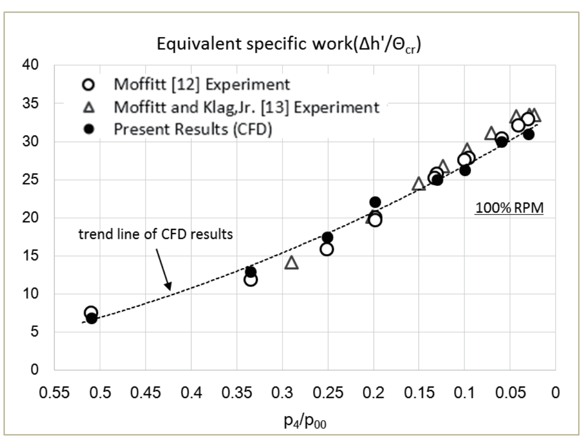

Fig. 6. Equivalent specific work output with turbine pressure ratio

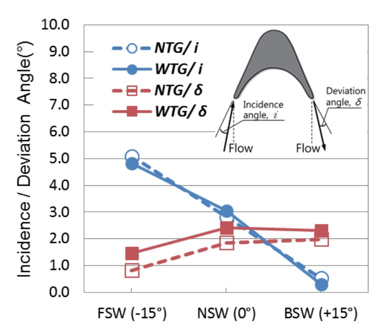

Fig. 7. Mass-averaged time mean incidence (i) and deviation (δ) angles

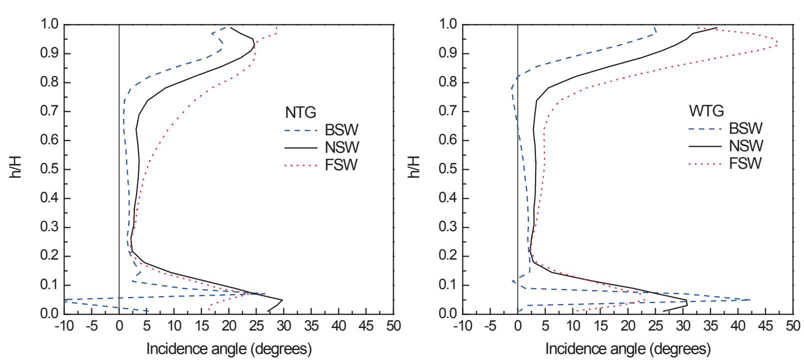

Fig. 8. Spanwise distribution of pitch-averaged mean incidence angles at rotor inlet

DOI: http://dx.doi.org/10.5139/IJASS.2015.16.4.571

span becomes higher compared with NSW model in both NTG and WTG case. By contrast, the incidence angles of the BSW model are more close to zero incidence angle and the span zone where the stream enters with analogous angle to zero incidence has also been formed more widely compared with NSW model. Change in incidence is more uniform for the BSW model along the span. This signifies that more losses induced by separation would occur in the fore part of a rotor passage at FSW and NSW cases because of relatively large flow angles compared with BSW model above the midspan.

Figure 9(a) ~ Fig. 9(f) show the time-averaged static pressure contours at nozzle outlet plane of all blade sweep models. The mean static pressure distributions at nozzle outlet plane are changed with rotor blade sweep angle. We can see the static pressure distribution increases in FSW model and decreases in BSW model compared with NSW model in both NTG and WTG cases. In particular, the conspicuous difference appears in upper part of the nozzle outlet. The difference usually occurs from a combination of factors, but it seems obvious that the rotor blade leading edge shock wave is one of these factors. As shown in Fig. 8, the incidence angles of three sweep models around 20% span are similar to each other, whereas those of FSW model are a lot bigger than the others around 75% span. Hence the leading edge shock wave propagates through axial gap spacing more toward the nozzle outlet in case of FSW model. In addition to that, the relatively short axial gap spacing over the midspan compared with other sweep models influences as well. For these reasons, the shock strength reached at upper part of nozzle outlet in FSW model is stronger and this raises the static pressure of nozzle outlet. If the static pressure of nozzle outlet increases more than design pressure, it makes shock wave inside the nozzle strong and eventually results in decrease of nozzle efficiency.

3.2 Sweep effect on the rotor blade passage.

Figure 10(a) and Fig. 10(b) show spanwise distributions of circumferentially averaged time-mean Mach number at rotor inlet (RI) and rotor outlet (RO) planes, respectively. First, Fig. 10(a) tells that the Mach number of BSW model is lower up to 15% span from the hub wall and higher above 15% span including the midspan region than NSW at RI plane. This lower Mach number region of BSW corresponds to the rotor hub overlap height. In case of BSW model, the axial gap distance becomes shorter as it's getting close to the hub wall. Hence, it is hard for flow to go into the rotor inlet after being diffused sufficiently near the hub region. In case of FSW model, the rotor inlet Mach number is lower than the other sweep models in almost the entire range of span. Because the static pressure values of three sweep models at nozzle outlet are different, as seen in Fig. 9, the nozzle outlet Mach number of BSW is higher and that of FSW is lower than that of NSW. Therefore, relatively lower Mach number at nozzle outlet influences on the hub region Mach number distribution of FSW model despite of long enough axial gap spacing.

Next, the features of Mach number distributions at RO plane are clearly revealed in Fig. 10(b). It could be found that the low Mach number regions of hub and tip blade overlap at RI plane are disappeared and the flows are spread out rather uniformly all over the span. The averages of rotor outlet Mach number of all sweep models are similar to each other but that of BSW model is slightly lower. As shown in Fig. 10 (b), the location of lowest Mach number in hub region rises toward midspan as the sweep angle becomes larger, i.e.

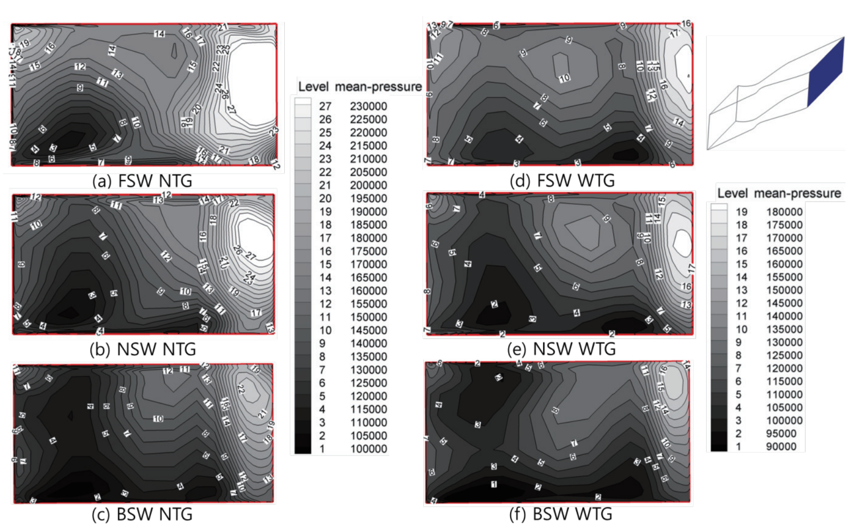

Fig. 9. Time-averaged static pressure contour at nozzle outlet

FSW → NSW → BSW. The Mach number distribution of BSW model is more uniform as a whole.

Figure 11(a) ~ Fig. 11(c) exhibit the time-averaged relative Mach number contours and stream lines of WTG case at 15%,

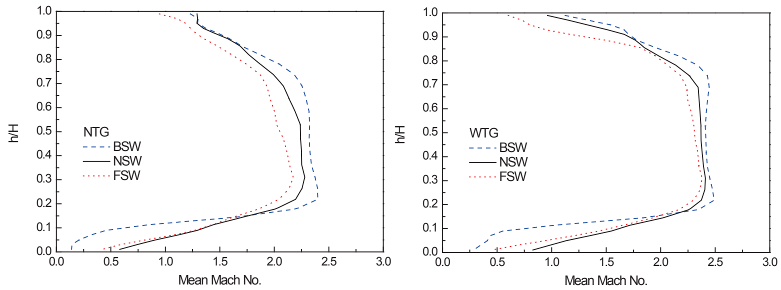

(a) Rotor Inlet

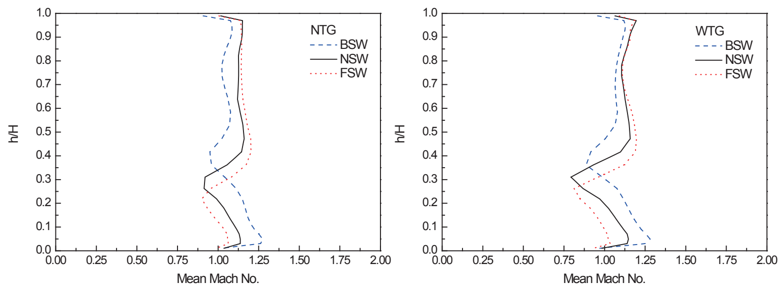

(b) Rotor Outlet

Fig. 10. Spanwise distribution of pitch-averaged mean Mach number

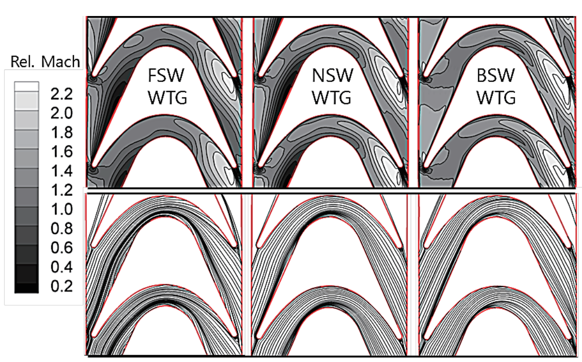

(a) 15% span

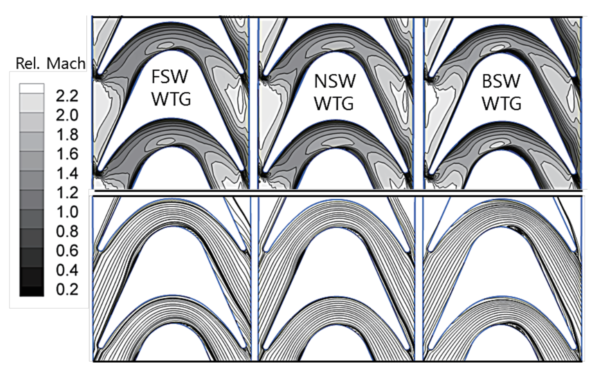

(b) 50% span

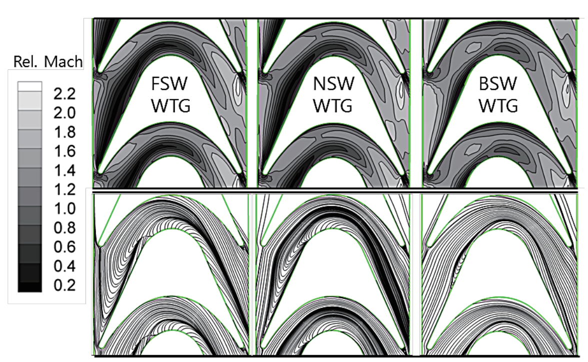

(c) 85% span

Fig. 11. Time-averaged relative Mach number contours and stream lines of WTG case

DOI: http://dx.doi.org/10.5139/IJASS.2015.16.4.571

50% and 85% span inside the rotor passage, respectively. In Fig. 11(a), there is no significant discrepancy of relative Mach number among those sweep models as seen in Fig. 9(a) but the suction surface separation and low velocity regions occurred in front of the 50% chord point are different in size. It is caused by different incidence angle as shown in Fig. 8. At 50% span and 85% span, the relative Mach number at rotor inlet becomes higher as the sweep angle increases, i.e. FSW → NSW → BSW. There is no separation bubble formed in front of the 50% axial chord at BSW model unlike the other models as shown in Fig. 11(b). On the other hand, the relatively high speed on the suction surface of BSW model leads flow separation with wider low velocity region on the suction surface behind the 50% blade chord.

In Fig. 11(c), extensive separated regions from leading edge on the suction surface are existed in FSW and NSW models. This is because of the axial gap spacing as well as the flow incidence angle mentioned above. In contrast to BSW model, the axial gap is not as wide as the flow coming from nozzle outlet spreads enough into the tip overlap region. In addition the shock waves occurred in front of rotor blade leading edge can reach to the nozzle outlet. And then the flow passed across these series of oblique shocks, which are relatively strong because they would not be dissipated yet, can be turned to the rotational direction.

3.3 Analysis of the blade loading

Figure 12 shows the time-mean static pressure distribution of the three sweep models at 15%, 50% and 85% span on the blade surface of NTG and WTG cases. The blade surface pressure distribution at 15% span illustrates that the loading near leading edge just after the stagnation point is a little bit reduced in BSW and is enhanced in FSW compared with NSW model. Except the vicinity of leading and trailing edge, the overall blade loading of BSW is increased compared with NSW in both of the NTG and WTG cases. Contrarily, the blade loading of BSW at 85% span near leading edge is increased in both of the NTG and WTG cases. The blade loading of FSW in NTG case around this region is a little bit enhanced while it is reduced in WTG case. Similarly, the overall blade loading of BSW at 85% span is also increased compared with the others.

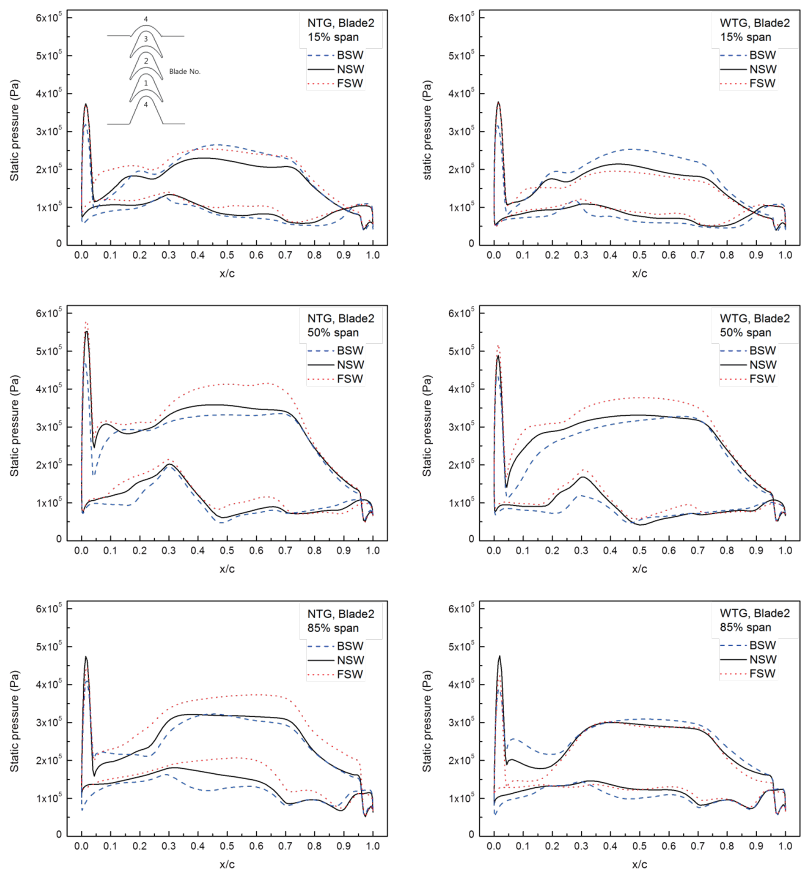

(a) NTG model (b) WTG model

Fig. 12. Time-averaged static pressure distribution on the blade surface

Denton et al. [6] referred the phenomenon like this in their research. They showed the blade loading near the lower wall was reduced near the leading edge and the opposite effect occurred near the upper wall in the backward swept turbine cascade. At the midspan, it can be shown the very rapid deceleration and acceleration along the suction surface in the front part of the 50% axial chord. These indicate the start point of separation bubble, reattachment location and the strength of passage oblique shock. In 50% span graph, the passage shock strength of BSW model is relatively weaker than NSW and FSW and the location of separation moves toward inside the rotor passage as the sweep angle increases. As same as the hub region result (15% span), the loading of BSW near the leading edge is reduced and vice versa in FSW model. The overall loading of BSW case is slightly reduced and that of FSW is enhanced compared to NSW. And it is observed that the peak point of blade loading in the vicinity of leading edge is getting away from the leading edge as the sweep angle increases. As a whole, the hub and tip loading was increased and the midspan loading was reduced in BSW model compared with NSW and the FSW model was vice versa.

3.4 Overall turbine performances

Figure 13 (a) ~ (d) show the contours of time-averaged entropy rise (Δs/R) and pitch-averaged values of time-mean Δs/R graphs along the span-wise direction at four specific locations of rotor passage. The entropy change in two properties of state can be calculated as follows by standard thermodynamic relations:

$$\frac{s - s_{ref}}{R} = \left(\frac{\gamma}{\gamma - 1}\right)\ln\left(\frac{T}{T_{ref}}\right) - \ln\left(\frac{P}{P_{ref}}\right) \quad (1)$$

Normally, P_{ref} and T_{ref} correspond to the total pressure and total temperature at the inlet.

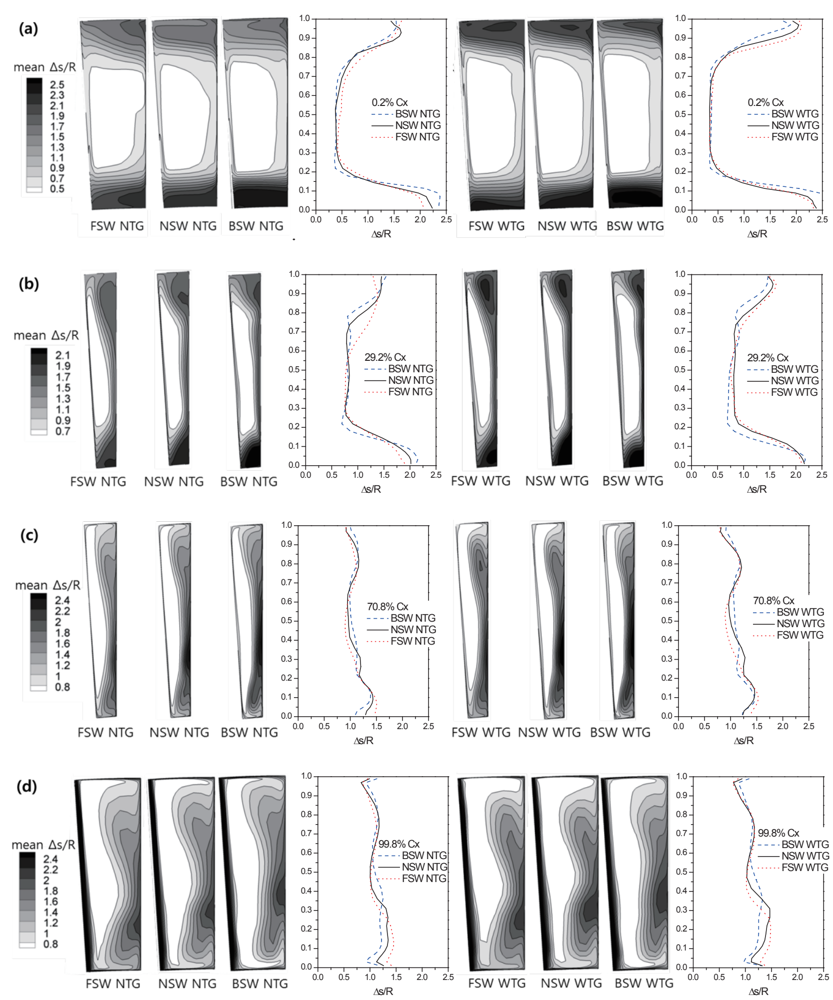

Fig. 13. Time-averaged Δs/R contour and spanwise plot of pitch-averaged mean Δs/R at (a) 0.2% (b) 29.2% (c) 70.8% (d) 99.8% of rotor blade axial chord

DOI: http://dx.doi.org/10.5139/IJASS.2015.16.4.571

As shown in Fig. 13 (a), when the sweep angle increases (FSW → NSW → BSW) the entropy rise values near-hub region become higher and those of near-tip region become lower at leading edge location. Fig. 13 (b) represents that the high loss part of near-tip region becomes wider and descends toward midspan through the rotor passage. The FSW model particularly shows higher entropy rise distribution compared with other two models in near-tip region at forepart of the blade. In Fig. 13 (c), as the main stream from nozzle outlet spread over the entire rotor passage, the entropy rise shows somewhat uniform distribution at 70% of blade axial chord.

In Fig. 13 (d), the entropy rise distribution reveals quite different aspect under about 60% span depending on the sweep model. In the hub region, up to about 30% span, the entropy rise of BSW model show lowest value among the sweep models while the entropy rise of FSW is higher than other two sweep models. But the BSW model produces entropy much more than the others in the vicinity of midspan. As for the region above the 80% span, the entropy rise of BSW is slightly bigger than that of the other models. In this figure, the spanwise locations of hub and tip passage vortices could be estimated roughly by the peak locations of entropy rise. As the sweep angle increases, the hub and tip passage vortex cores move toward positive radial direction and the extent of movement is more notable at the hub passage vortex. Although the sweep cases showing a best performance are each different depending on the per cent span, both graphs indicate that the BSW model has better performance compared with NSW and FSW models in the region from hub to about 30% of rotor span.

In the meantime, the tip leakage mass flow rate through rotor tip gap depending on the three sweep models showed a remarkable difference in case of WTG model. The leaking flow would lead to an additional entropy rise by mixing process between the leakage flow and the main flow in downstream of the blade rows. As a result of the calculations, the tip leakage mass flow rate of BSW model shows about 71% value of NSW model and that of FSW model shows about 121% value of NSW model.

Table 1 presents the time-mean overall total-to-static turbine efficiency calculated at MO plane of all sweep cases.

Table 1. Efficiency at MO Plane

		FSW (-15°)	NSW (0°)	BSW (+15°)
NTG	η_{tt} (%)	56.6	57.4	57.7
	η_{ts} (%)	44.6	45.3	45.8
WTG	η_{tt} (%)	53.3	54.5	56.1
	η_{ts} (%)	43.4	44.0	44.9

The turbine efficiency equations used here are as follow:

$$\eta_{tt} = \frac{1 - T_{03}/T_{01}}{1 - (P_{03}/P_{01})^{\frac{\gamma-1}{\gamma}}} \cdot 100 \tag{2}$$

$$\eta_{ts} = \frac{1 - T_{03}/T_{01}}{1 - (P_{3}/P_{01})^{\frac{\gamma-1}{\gamma}}} \cdot 100 \tag{3}$$

As shown in this figure, the efficiency of BSW model is higher than the efficiency NSW model and the efficiency of FSW model is lower than that of NSW model in both NTG and WTG cases. There was a total to static efficiency change of +0.5% for BSW model and -0.7% for FSW model versus NSW model in NTG case. In case of WTG, there was an efficiency change of +0.9% for BSW model and -0.6% for FSW model versus NSW model. The total to total efficiency in WTG case showed prominent results. The total efficiency of BSW model increased 1.6% and that of FSW model decreased 1.2% model compared with NSW model.

4. Conclusion

Rotor blade sweep of a small axial supersonic impulse turbine has been considered as a method to improve turbine performance. Unsteady three-dimensional Navier-Stokes simulations have been performed on nozzle and rotor blade rows corresponding to 1/25 annulus and the results are compared with each other. Relative flow angles, Mach number distributions, flow patterns, blade loadings, entropy rise, and turbine efficiency have been analyzed.

Following conclusions can be drawn,

1. The incidence angle at rotor inlet plane tends to reduce as the sweep angle increases. The BSW, the positive sweep angle model, was consequently shown the best result among the three sweep models.
2. The Rotor blade sweep can affects the average Mach number and its distribution over the rotor passage. The inlet Mach number becomes higher when the sweep angle becomes larger. The low velocity peak location of rotor outlet moves toward the midspan as the sweep angle increases.
3. With the blade static pressure distribution result, it was possible to understand the blade loading distribution, shock location, relative strength and the extent of loss in the vicinity of hub, midspan and tip, approximately. Consequently, the BSW model showed increased hub and tip loading and decreased midspan loading compared to NSW. The FSW model was vice versa.
4. The sweep angle had a considerable effect on the mass

flow rate of leakage flow through tip gap in WTG case calculation. According to the calculation result, the tip leakage mass flow rate of BSW model shows about 71% value of NSW model and that of FSW model shows about 121% value of NSW model.

5. The flow loss in the region from hub wall to about 30% span of BSW model is less than the other models. And the BSW model also showed increase in overall turbine efficiency compared with NSW model.

Acknowledgement

This work was supported by a 2-Year Research Grant of Pusan National University.

References

[1] Lewis, R. and Hill, J., "The Influence of Sweep and Dihedral in Turbomachinery Blade Rows", *Journal of mechanical Engineering Science*, Vol. 13, No. 4, 1971, pp.266-285. DOI:10.1243/JMES_JOUR_1971_013_043_02

[2] Hill, J. and Lewis, R., "Experimental Investigations of Strongly Swept Turbine Cascades with Low Speed Flow", *Journal of mechanical Engineering Science*, Vol. 16, No. 1, 1974, pp. 32-40. DOI:10.1243/JMES_JOUR_1974_016_007_02

[3] Denton, J. and Xu, L., "The Exploitation of Three-dimensional Flow in Turbomachinery Design", *Proceedings of the Institution of Mechanical Engineers, Part C, Journal of Mechanical Engineering Science*, Vol. 213, No. 2, 1999, pp. 125-137. DOI:10.1243/0954406991522220

[4] Wadia, A., Szucs, P. and Crall, D., "Inner Workings of Aerodynamic Sweep", *ASME Journal of Turbomachinery*, Vol. 120, 1998, pp. 671-682. DOI:10.1115/1.2841776

[5] Gümmer, V., Wenger, U. and Kau, H., "Using Sweep and Dihedral to Control Three-Dimensional Flow in Transonic Stators of Axial Compressors", *ASME Journal of Turbomachinery*, Vol. 123, 2001, pp. 40-48. DOI:10.1115/1.1330268

[6] Denton, J., "The Effects of Lean and Sweep on Transonic Fan Performance: A Computational Study", *TASK QUARTERLY*, Vol. 6, No. 1, 2002, pp. 7-23.

[7] Pullan, G. and Harvey, N. W., "Influence of Sweep on Axial Flow Turbine Aerodynamics at Midspan", *ASME Journal of Turbomachinery*, Vol. 129, No. 3, 2007, pp. 591-598. DOI:10.1115/1.2472397

[8] Pullan, G. and Harvey, N. W., "Influence of Sweep on Axial Flow Turbine Aerodynamics in the Endwall Region", *ASME Journal of Turbomachinery*, Vol. 130, No. 4, 2008, pp. 041011-1~041011-10. DOI:10.1115/1.2812337

[9] Yoon, S., Denton, J., Curtis, E., Longley, J. and Pullan, G., "Improving Intermediate Pressure Turbine Performance by Using a Nonorthogonal Stator", *ASME Journal of Turbomachinery*, Vol. 136, No. 1, 2014, pp. 021012-1~021012-8. DOI:10.1115/1.4023941

[10] Hah, C. and Shin, H., "Study of Near-Stall Flow Behavior in a Modern Transonic Fan with Compound Sweep", *ASME Journal of Fluid Engineering*, Vol. 134, 2012, pp. 071101-1~071101-7 DOI:10.1115/1.4006878

[11] Menter, F. R., "Two-Equation Eddy-Viscosity Turbulence Models for Engineering Applications", *AIAA Journal*, Vol. 32, No. 8, 1994, pp. 1598~1605. DOI:10.2514/3.12149

[12] Moffitt, T. P., "Design and Experimental Investigation of a Single-Stage Turbine with a Rotor Entering Relative Mach Number of 2", NACA RM E58F20a, 1958.

[13] Moffitt, T. P. and Klag, F. W., Jr., "Experimental Investigation of Partial- and Full-Admission Characteristics of a Two-Stage Velocity Compounded ", NASA TM X-410, 1960